Soft Matter

PAPER

View Article Online
View Journal | View Issue

Cite this: *Soft Matter*, 2022, **18**, 9291

Soft electrochemical bubble actuator with liquid metal electrode using an embodied hydrogel pneumatic source†

Veenasri Vallem, [a] Erin Roosa,[a] Tyler Ledinh,[a] Sahar Rashid Nadimi, [ab] Abolfazl Kiani [ab] and Michael D. Dickey *[a]

Received 29th June 2022,
Accepted 22nd November 2022

DOI: 10.1039/d2sm00874b

rsc.li/soft-matter-journal

Soft pneumatic actuators—such as those used for soft robotics—achieve actuation by inflation of pneumatic chambers. Here, we report the use of the electrochemical reduction of water to generate gaseous products that inflate pneumatic chambers. Whereas conventional pneumatic actuators typically utilize bulky mechanical pumps, the approach here utilizes only electricity. In contrast to dielectric actuators, which require ~kV to actuate, the electrochemical approach uses a potential of a few volts. The applied potential converts liquid water—a safe, abundant, and cheap fuel—into hydrogen gas. Since the chambers are constructed of hydrogel, the body of the actuator provides an abundant supply of water that ultimately converts to gas. The use of liquid metal for the electrode makes the entire device soft and ensures intimate contact between the chamber walls and the electrode during inflation. The device can inflate in tens of seconds, which is slower than other pneumatic approaches, but much faster than actuating hydrogels *via* principles of swelling. The actuation volume can be predicted and controlled based on the input parameters such as time and voltage. The actuation shape and position can also be controlled by the position of the electrodes and the geometry of the device. Such actuators have the potential to make tether-less (pump-free), electrically-controlled soft devices that can even operate underwater.

1. Introduction

This paper describes the fabrication and characterization of a soft electrochemical bubble actuator. The term 'bubble' is commonly used to describe a small body inflated with gas. Many species in nature generate or use bubbles to perform actions ranging from breathing to hunting prey. For example, bubbles are used to breathe (diving bell spider), smell (star-nosed mole), find prey (pistol shrimp), protect from predators (spittlebug), and even raft (violet snail).[1] Likewise, researchers have been using bubbles to perform activities from regulating fluid flow[2] to killing cells selectively.[3] Bubbles also find use in micro-valves[4] and pumps,[5] micromanipulators,[6] dynamic lenses,[7] tactile sensing,[8] actuators like artificial muscles,[9] and soft robotics.[6,10]

Colloquially, the term bubbles usually refer to small volumes of gas surrounded by a liquid; here we use the term 'bubble' more generally to describe elastic chambers filled with gas. Bubbles formed from liquids (or solids) are appealing as actuators because of the enormous change in volume. For example, 1 mol of water increases volume by ~1244 times when converted to water vapor at room temperature. Such large changes in volume find use in commercial products, such as airbags for cars. Gas can be generated by (i) heating liquid to form vapor (phase change actuators),[3] (ii) electrochemically displacing microscale elastic membranes[2,4] or fluid (electrochemical actuators)[5] (iii) injecting air into expandable chambers (pneumatic actuators)[9,11] and (iv) applying electrostatic forces to deform a fluid-filled elastomer chamber (dielectric actuator).[7,8] Here, we generate the gas electrochemically to actuate elastomeric chambers composed of a hydrogel.

Pneumatic actuation of elastomeric chambers is commonly used for soft robotics. Such chambers are lightweight and easy to fabricate. They can also provide non-linear motion with simple inputs and use soft materials that interact safely with humans.[12] Generally, pneumatic actuators convert electrical energy (from an outlet or battery), to mechanical energy (pumping), and ultimately to pneumatic energy (PV work) that actuates the device. Unfortunately, the pumps used to inflate the chambers are bulky and use tubing that "tethers" the devices, thus limiting their motion. There are exceptions;

[a] *Department of Chemical and Biomolecular Engineering, North Carolina State University, Raleigh, NC, 27695, USA. E-mail: mddickey@ncsu.edu*
[b] *Department of Chemistry and Biochemistry, California State University, Bakersfield, Bakersfield, CA, 93311, USA*

† Electronic supplementary information (ESI) available. See DOI: https://doi.org/10.1039/d2sm00874b

chemical reactions can rapidly generate pressure without the need for pumps, but use potentially dangerous explosions.[13,14] We were motivated to explore ways to inflate pneumatic chambers without a pump and in a way that could be inflated directly with electricity using safe materials. Although dielectric actuators function based on electrical input, they require very high voltages (~kV) to actuate.[15] In contrast, electrochemical actuators require only a few volts (~V) to actuate.[4]

The electrochemical actuators used here consist of two electrodes in a hydrogel. The hydrogel serves as an electrolyte medium. Upon applying a voltage between the electrodes, redox reactions occur at the interface between the hydrogel and electrode. One or more of the reactions produce gaseous products depending on the design. The most relevant prior work utilized liquid electrolytes packed in a microscale elastomeric chamber with rigid electrodes.[4] Such actuators were used for small-scale (μm) actuation and not soft robotics. We show here that rigid wires are poorly suited for larger (cm scale) devices because the inflation of the chambers separates the hydrogel and the wire. Electrodes that maintain contact with the hydrogel are necessary for proper pneumatic inflation in our design.

We report an entirely soft electrochemical bubble actuator made of liquid metal (LM) electrodes and hydrogel. LM electrodes composed of gallium alloys (here, eutectic gallium indium) have been interfaced with hydrogel before for electrodes,[16] energy harvesting,[17] and memory devices,[18] but not for the purpose of driving electrochemical reactions for bubble actuators. Here, the hydrogel serves two purposes: (1) it forms stretchable chambers that can inflate pneumatically, and (2) it contains water ~70% water, which serves as the 'fuel' for electrochemical actuation. Applying voltage to the LM converts the water from the hydrogel—which is biocompatible and inexpensive—into hydrogen gas. The gas formed inflates the hydrogel membrane forming a bubble that contains hydrogen gas, LM, and a small amount of water from the wall of the hydrogel. Thus, we use the term 'bubble' to describe the gas formed[19] and the term 'chamber' to describe the entire bubble including the hydrogel walls that encase the bubble. The word 'chamber' is also used to distinguish between the liquid based electrochemical actuators where liquid electrolyte is filled in an elastic sac, while here, the chamber wall (gel in contact with the LM) provides the electrolyte for actuation. Thus, the pneumatic fuel (water) is 'embodied' within the walls of the hydrogel chamber.

The devices can undergo multiple actuation cycles as very little water is consumed per cycle. In principle, such hydrogels can even absorb water from the environment to provide continuous operation.[20] The soft LM electrode stays in contact with the hydrogel, which is necessary to form the hydrogen gas continuously. The actuator requires only a few volts of voltage input and actuates within seconds. The actuator retains 60% of the bubble volume for 6 h upon removing the voltage input. Although not a focus here, the design can also be modified to enable reversible actuation, which allows the hydrogel membrane to expand and contract within a few seconds. We characterized the performance of these devices as a function of counter electrode material, input voltage, and device architecture. The actuation volume can be predicted based on the input parameters such as time and voltage. In addition, we studied various device architectures to induce curvature in the system upon bubbling to create hydrogel grippers. To our knowledge, this is the first report of macroscale (~cm) soft electrochemical actuators where the chamber wall provides the electrolyte for actuation.[21] These devices provide pump-free and electronically controlled actuation of soft hydrogel-based devices. Here, we introduce the concept of using soft electrochemical systems that could enable pump-free pneumatic actuation. We characterize the bubbling mechanism by varying the input voltage, time, and distance between the electrodes. We also demonstrate ways to induce curvature in the system that could help perform actions like lifting objects.

2. Results and discussion

The electrochemical bubble actuator consists of two liquid metal droplets that serve as electrodes while the hydrogel acts as a source of electrolyte (Fig. 1A). The use of LM, rather than solid metal electrodes, ensures the entire device is soft.[22] When applying a voltage across the two electrodes, redox reactions occur at the two electrodes. At the anode, gallium undergoes oxidation, causing the surface to appear grey due to the formation of gallium oxide[18,23] (right electrode in Fig. 1B). We did not observe any bubbling at the anode however, we note that there could be chlorine and oxygen gas formation at the anode. At the cathode, there are two reactions. First, the thin native oxide on the surface of the LM electrode reduces. This causes the metal to retract into a sphere due to the high surface tension of liquid metal[24,25] (left electrode in Fig. 1B). The movement of the metal minimizes the surface area of the metal, and this movement effectively creates a chamber in the hydrogel that ultimately gets inflated by gas. Gas forms when the hydrogel reduces to form hydrogen gas *via* $2H^+ + 2e^- \rightarrow H_2$. The gas continues to form while applying the potential and inflates the chamber (Fig. 1B and C). For example, when a voltage of 15 V is applied across the LM electrodes for 30 seconds, the bubble inflates the hydrogel cavity from 22.5 mm^3 (defined by the volume of the LM electrode) to a volume of 818 mm^3.

Gas formation is enhanced by the use of LM due to its ability to flow to maintain contact with the gel. Upon applying a reducing potential to devices fabricated using only Cu electrodes (Fig. 1D), a thin layer of gas formed around the electrode (Fig. 1E), causing the electrode to lose contact with the hydrogel. Hence, the chamber did not grow further in the absence of liquid metal, as shown in ESI,† Video S1. Applying 15 V for 20 s to the copper electrodes creates insignificant inflation (Fig. 1F) compared to the device made of LM electrodes (Fig. 1C). We also tried to contact the hydrogel chamber with other stretchable electrodes, such as arrays of silver nanowires, but the nanowires quickly degraded in the electrochemical environment.

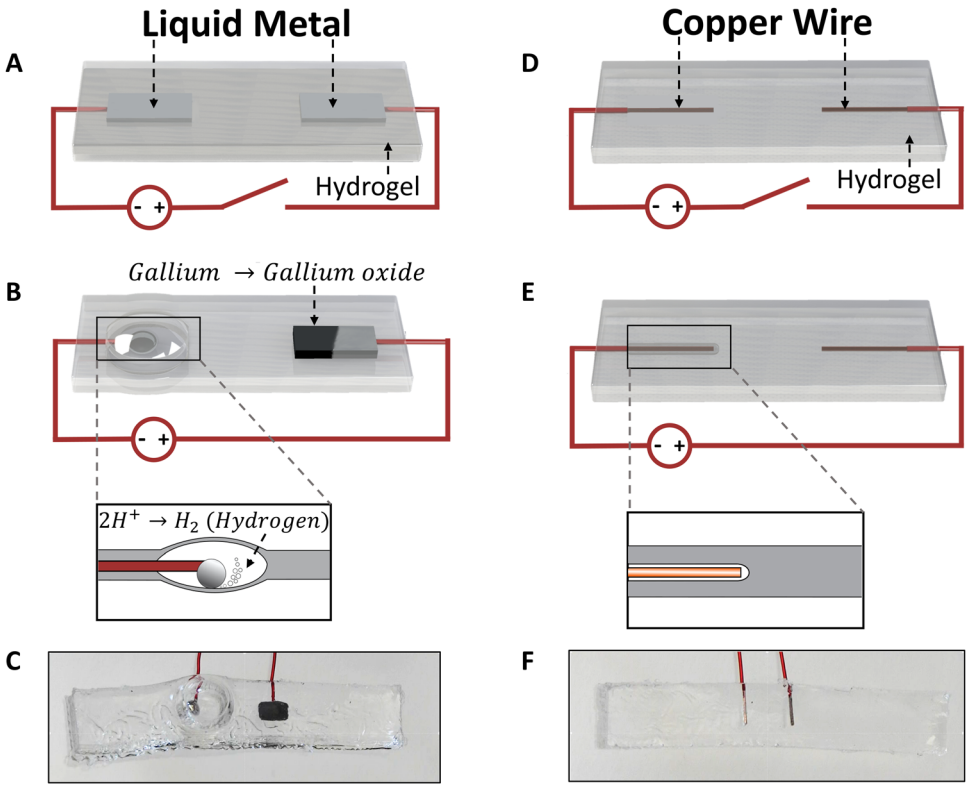

Fig. 1 A comparison of soft and stretchable electrochemical bubble actuators made using liquid metal (left column) or copper electrodes (right column). (A) Bubble actuator made of LM electrodes and hydrogel. (B) When a voltage is applied, one electrode reduces causing the LM to retract into a sphere due to high surface tension upon reducing the native oxide layer. The other electrode oxidizes *via* the formation of thicker, grey gallium oxide. The bare metal then reduces the water in the hydrogel, generating hydrogen gas. Due to its fluidity, the LM does not lose contact with the hydrogel. Thus, the reduction reaction continues, and the chamber inflates *via* the formation of a bubble. (C) Picture of an LM-hydrogel actuator with an inflated chamber after 20 s of gas formation at 15 V. (D) Bubble actuator made of traditional rigid electrodes (copper). (E) As water from the hydrogel reduces to hydrogen gas, a thin gas pocket forms around the copper electrode, causing it to detach from the gel and therefore stop producing more gas. (F) Picture of copper wire-hydrogel actuator after 20 s at 15 V. The actuators showed in C and F are 5.5 cm in length.

We used polyacrylamide gel because it is soft, stretchable, and easy to fabricate by simple photopolymerization of a monomer solution (see Experimental section). We used 1.5 mm thick walls as it enables actuation within seconds and retains the bubble volume for several hours. For example, a bubble formed upon inflating for 30 seconds at 10 V input retains 60% of the volume for 6 h after ceasing to apply voltage (ESI,† Fig. S1).

The use of LM and hydrogel in making electrochemical actuators provides the following unique attributes:

1. LM and hydrogel are both inherently soft and therefore help realize soft and deformable actuators.

2. Conventional metal wires lose contact with the gel due to the thin pocket of gas that forms during actuation. In contrast, the LM stays in contact with the hydrogel, which is necessary to continuously form the gas that inflates the chamber.

3. The gas forms from water, which is safe, abundant, and inexpensive.

4. The hydrogel chamber walls, which contain ~70 wt% water, provide the 'embodied' source of water.

5. The devices can undergo multiple actuation cycles since very little water is consumed per actuation (ESI,† Video S2).

6. Although actuation is much slower than pump-based pneumatic actuators, the actuation takes place in seconds, which is faster than hydrogel-based actuators that utilize diffusion of water in or out of the gel to cause swelling (minutes to hours).[26,27]

7. The LM starts out as a rectangular shape but retracts into a sphere during reduction creating a void that directs the chamber shape. This allows a facile route to regulate the geometry of the chamber (ESI,† Video S3).

2.1. Bubble actuator characterization

We characterized the performance of the device (bubble volume) as a function of the parameters highlighted in Fig. 2A: time and voltage.

The volume of the hydrogen bubble can be calculated using the ideal gas law,

$$\text{Bubble volume}\ (t) = N(t)RT/P(t) \quad (1)$$

where N is the number of moles, R is the gas constant, T is the temperature and P is the pressure. The generic symbol $X(t)$ implies 'X' at a time 't'. The number of moles of the gas relates

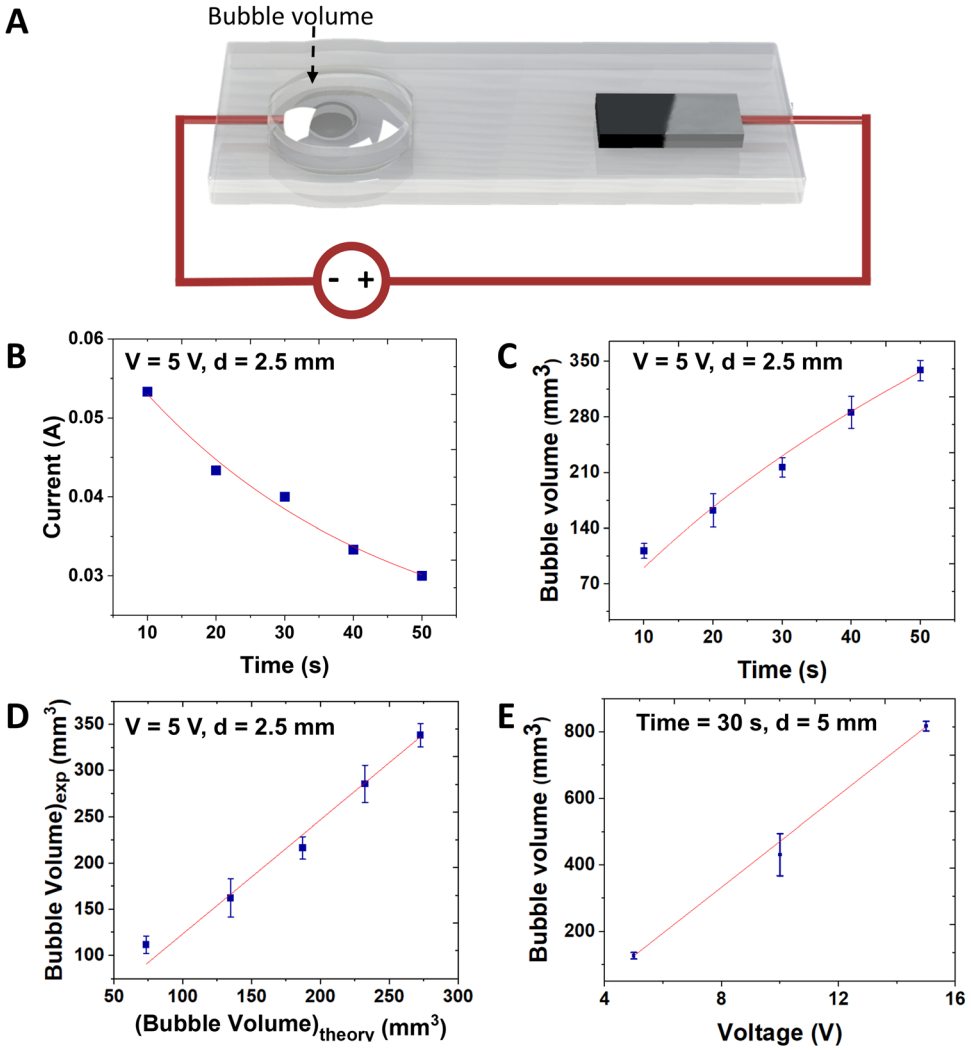

Fig. 2 Bubble actuator characterization. (A) A schematic describing the input and output parameters. (B) The current generated in the bubble actuator system and (C) the output (bubble volume) measured as a function of time while applying 5 V. (D) Comparison of experimental and theoretical model results, which are fit with a line with a slope of 1.23 and R^2 = 0.998. (E) The bubble volume measured as a function of voltage applied. The bubble volume was recorded at 30 s in each case while a corresponding voltage was applied. The error bars are generated by analyzing the readings from three different devices. The red lines indicate model predictions of the output parameter (dependent variable on y – axis) based on the input (independent variable on x – axis). The distance between the electrodes in the bubble actuator in B, C, D, is 2.5 mm and E is 5 mm. For further details on the role of the distance between the electrodes, see ESI,† Fig. S2.

to the current, as shown in eqn (2),

$$N(t) = \frac{Q}{nF} = \frac{\int_0^t i(t)\mathrm{d}t}{nF} \quad (2)$$

where Q is the charge generated, n is the number of electrons transferred during oxidation/reduction, F is the Faraday constant, and i is the current.

The volume expansion of the chamber is opposed by two forces: (1) the surrounding atmospheric pressure, and (2) the elasticity of the walls of the hydrogel chamber. We find that the elasticity of the walls is negligible due to the low modulus and thin nature of the gel (scaling relations are found in the ESI†). Thus, to simplify the analysis, we approximate the pressure to be constant and approximately equal to P_{atm}. Thus,

$$\text{Bubble volume } (t) = D \times \int_0^t i(t)\mathrm{d}t \quad (3)$$

where D is a constant equal to RT/nFP_{atm}.

Eqn (3) requires knowledge of the current, which we measured simultaneously during inflation as plotted in Fig. 2B. We fit the data with exponential decay. The Randles equivalent circuit is often used to predict the current response of an electrochemical system to a step change in voltage.[28,29] Although the Randles model predicts an exponential decay, the premise of the model does not capture all the physical changes occurring here, such as changes to the shape and contact area of the electrodes. Nevertheless, the data nicely fits to an exponential decay (eqn (4)), which suits the purpose of

having a mathematical prediction of current *versus* time to satisfy eqn (3).

$$i(t) = A + B\exp(-t/\tau) \quad (4)$$

The red line in Fig. 2B indicates the best fit using eqn (4).

Role of time. Fig. 2C shows that, as expected, the volume of the bubble increases with time while applying 5 V. To obtain a prediction for the bubble volume, we plug eqn (4) into eqn (3) and perform the best fit by varying the parameter D as the only fitting parameter (ESI†). The fit, as indicated by the red trace in Fig. 2C, captures the trends of the experimental data, suggesting this scaling captures the dynamics of the system with respect to time.

Fig. 2D plots the experimental chamber volume *versus* the theoretical bubble volume data. The latter is obtained by using $D = RT/nFP_{atm} = 126$, slightly smaller than the empirical fit of $D = 156$. A linear fit gives a slope of 1.23 and $R^2 = 0.998$, intercept 0. A slope greater than 1 suggests that the experimental volume increases more than expected from the theory. This discrepancy could be due to the challenges associated with estimating the bubble volume. We assume the bubble is an ellipsoid. We determine the bubble volume by measuring the diameters of the ellipsoid manually from the side and top view pictures using Image J software. Thus, there could be error (for more details, see ESI†).

Role of voltage. The volume of the bubble increases linearly with voltage as shown in Fig. 2E. For each data point in the graph, the corresponding voltage is applied for 30 seconds. The chamber only inflates above 3 V (ESI,† Fig. S3). For bubble volume as a function time at each voltage, see ESI,† Fig. S4.

2.2. Curvature

In a two LM electrode system (*cf.* Fig. 1), an irreversible oxidation reaction at the surface of the anode results in a dark grey colored gallium oxide. The dark grey-colored residue is observed previously in systems that use sodium chloride solution.[30] The oxide buildup can increase the resistance of the device. To avoid the oxide residue, we used carbon felt as an anode. The oxygen formed at the anode diffuses out of the device through the pores in the carbon felt electrode since it is attached to the external surface of the hydrogel, that is, one side of the carbon felt is attached to the hydrogel and the other side is open to the air (see Experimental methods section). Hydrogen formed at the cathode is captured inside the gel resulting in a bubble. The use of carbon felt has another advantage as it breaks the mechanical symmetry of the device and causes the device to bend out of the plane during actuation (Fig. 3). Thus, the actuated hydrogels experience a strain gradient across the top and bottom layers as the top layer extend because of the bubble formation, creating curvature in the hydrogel (for bending angle as function of time, see ESI,† Fig. S5). The actuation shape and position can also be controlled by the position of the counter electrode and the LM pattern (ESI,† Fig. S6) presenting a wider scope for controlled actuation.

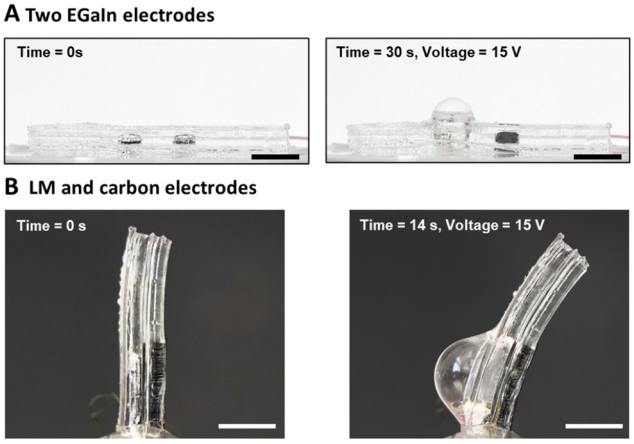

Fig. 3 Bubble actuator and curvature. Photographs of the bubble actuators made with (A) two LM electrodes at time 0 and 30 s upon applying an input voltage of 15 V, and (B) one LM and one carbon electrode at time 0 and 14 s upon applying an input voltage of 15 V. The scale bars represent 1 cm.

2.3. Grippers

Using the curvature generated in the LM-carbon electrode system we demonstrated two ways to assemble a bubble actuator gripper as shown in Fig. 4. In Fig. 4A, the LM electrodes are located on the exterior of the device (away from the object) thus inducing an inward curl (Fig. 4B). In Fig. 4C, the LM electrodes located on the interior of the device (in proximity to the object) induce an outward curl (Fig. 4D). The grippers required 10 V for 30 s and 16 s, respectively, to grasp the objects. This time scale is slower than using a pneumatic pump, but it is much faster than other hydrogel actuators that rely on osmotic pressure to actuate.

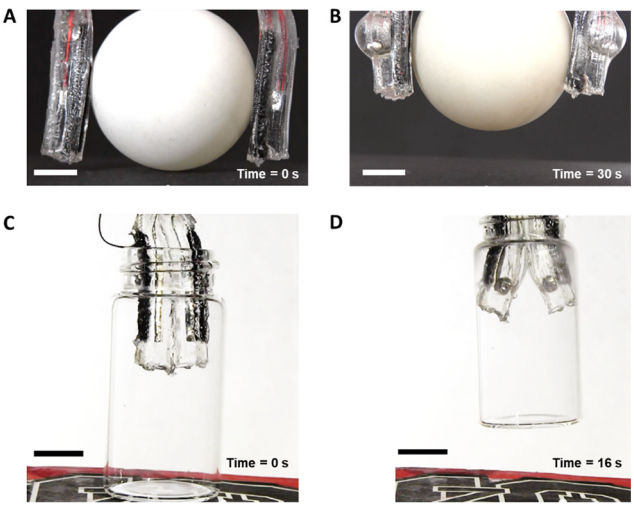

Fig. 4 Bubble actuator gripper. Photographs demonstrating the two modes of gripping: (A and B) inward curl gripping and (C and D) outward curl gripping. The grippers held the objects firmly after lifting them off the ground (B) a ball of 4 cm diameter and (D) a 20 ml glass vial in 30 s and 16 s respectively when a voltage input of 10 V is applied. The demonstrations can be found in ESI,† Videos S4 and S5. The scale bars represent 1 cm.

Actuator performance. From this initial study, we provide simple numerical estimations to describe the actuator performance. The bubble actuator here generates a force sufficient to inflate the walls of the chamber. With a gel modulus of 40 kPa, a chamber wall thickness of 1.5 mm, and a strain of $\sim$0.45, the force generated is on the order of 1 N. The power efficiency is $\sim$1% based on the PV (pressure–volume) work relative to the input electrical power (current $\times$ voltage $\times$ time). Overall, the actuator performance – force of 1 N (for the geometry used here), actuation stress of 18 kPa, and energetic efficiency of 1% – is comparable to the other soft actuators including hydrogels,[31] pneumatics,[32] electroactive polymers,[33] and flexible 2D electrodes.[34] The force generated is also comparable to natural passive hydraulic actuators.[35]

3. Conclusion

We report electrochemical bubble actuators built from liquid metal and hydrogel. In addition to making the device soft, the use of liquid metal ensures intimate contact between these electrodes and the walls of the hydrogel chamber. The hydrogel serves as a source of water, which reduces to hydrogen at low voltage (5–10 V). The resulting hydrogen gas inflates the chambers in tens of seconds, which is slower than pneumatic pumps but faster than hydrogel actuators that utilize swelling. It also eliminates the need for pneumatic tubing that tethers soft actuators and provides a mechanism to actuate directly using electricity. We show these actuators can grip objects gently. Here we use a power supply to drive the electrochemistry, but note that recent literature suggests ways of embodying energy sources within actuator bodies.[36]

The actuator retains 60% of its final bubbled state for 6 h upon removing the voltage input. A focus of ongoing and future work is to design vents to enable reversible actuators. For example, our initial results suggest the design can also be modified to enable reversible actuation by venting the gas at a rate that varies non-linearly with inflation. This would allow the hydrogel membrane to expand and contract within a few seconds (ESI,† Video S2). In principle, the hydrogen could also be used further, either as a fuel (for combustion-based actuation) or to simply recombine with oxygen to regenerate the water. Although we did not show it here, gels can be made to be hygroscopic, and thus, it may be possible to harvest additional water from the atmosphere to replace consumed water.[20]

We characterized the performance of these devices as a function of electrode material, input voltage, and device architecture. We modeled the behavior to show that the actuation volume as a function of time is directly proportional to current. For the gels used here, the current increases with voltage and by decreasing the distance between the electrodes. In addition, we studied various design architectures to induce curvature in the system upon bubbling and demonstrated hydrogel grippers. To our knowledge, this is the first macroscale (cm) soft electrochemical actuator reported. These devices with pump-free and electronically controlled actuation may find use in enabling autonomous soft grippers or haptics. In addition, the unique combination of materials allows a new type of hydrogel actuators that are soft, biocompatible, and can operate underwater.

This work demonstrates a way to use soft electrochemical systems in enabling pump-free pneumatic actuators. There remain challenges and opportunities: (1) establishing reversible actuation using effective mechanical designs and/or novel chemistry. (2) Optimizing the actuator performance such as blocked force and speed by varying the materials of construction and geometry. (3) Limiting water loss from the hydrogels. (4) Identifying chemistries that enable faster actuation, require lower input voltage, and avoid irreversible reaction products that cause active material loss such as electrodes and electrolyte during actuation.

4. Experimental section

4.1. Materials

Liquid metal, eutectic mixture of gallium and indium (EGaIn), was purchased from Indium Corporation. Acrylamide, 2-hydroxy-4′-(2-hydroxyethoxy)-2-methylpropiophenone (Irgacure 2959), *N*,*N*′-methylenebis(acrylamide) (MBA) were purchased from Sigma Aldrich. Sodium chloride (NaCl) was purchased from Fisher Scientific. Carbon felt (0.125 in thick) was purchased from Alfa Aesar by Thermo Fisher Scientific. Customized molds used to fabricate devices are made from acrylic sheets. A laser writer (Universal laser systems VLS 3.5) was used to cut the sheets into desired shapes as described in our previous work.[17]

4.2. Fabrication of liquid metal–hydrogel energy generator

We fabricated the liquid metal–hydrogel composites using a three-step process as described in our previous work.[17] We describe the process here for convenience. ''We used acrylamide pre-gel solution (30% w/v acrylamide (monomer), 0.04% w/v MBA (crosslinker), 0.13% w/v irgacure 2959 (initiator)) to make the hydrogel. Besides the materials that make the polymer network, we add NaCl to the pre-gel solution to make a concentration of 1 M for enhancing the conductivity of the gel. First, we cured the pre-gel solution in an acrylic mold using a 55 mW cm^{-2} intensity UV lamp for 4 min to make a hydrogel. Second, we filled liquid metal in the molded voids. Finally, more pre-gel was cured to encase the liquid metal. The fabricated liquid metal–hydrogel composites are soft and stretchable up to 400%. The gels used in this study are 6 mm thick, 5.5 cm long, and 1 cm in width unless mentioned otherwise.''

To attach a carbon felt electrode, we follow slightly different fabrication steps. First, we place the carbon felt electrode on the bottom of the mold and pour the pre-gel solution on the top and cure it so one side of the carbon felt is open to the air and the other side is covered with the gel. In parallel, we follow the first and the second steps mentioned above to obtain a hydrogel with pockets filled with LM. Later, we pour a few drops of pregel solution on top of that and place the carbon-felt gel

composite with carbon felt facing the air. We then cure it to bind both gels.

4.3. Characterization

We applied a voltage to the liquid metal–hydrogel actuator using an Extect or Tacklife MDC01 DC Power supply to the system. Videos were taken of the hydrogels as they inflated from the side view and the top view, and images taken from the videos at certain time intervals were analyzed in ImageJ. The volume of the bubble formed at the cathode was calculated using the equation for the volume of an ellipsoid.

$$\text{Bubble volume} = \frac{2}{3}\pi abc$$

Bubble volume is estimated using the volume equation for an ellipsoid, where a was the x-radius of the ellipsoid and b was the y-radius of the ellipsoid, and c was the height of the ellipsoid. a and b are obtained from the top view photograph and c is obtained from the side view photographs as shown in ESI,† Fig. S7. We limit the experimental time to 50 s to prevent bubble bursting.

Author contributions

Conceptualization, V. V., and M. D. D.; investigation, V. V., E. R., and T. L.; methodology, V. V., S. R., A. K., and M. D. D.; validation, E. R., T. L.; writing—original draft preparation, V. V., E. R., and T. L.; writing—review and editing, V. V., M. D. D.; supervision, M. D. D.; funding acquisition, M. D. D.

Conflicts of interest

There are no conflicts to declare.

Acknowledgements

The authors gratefully acknowledge support from the National Science Foundation ASSIST ERC (ASSIST, EEC-1160483) and the Coastal Studies Institute of North Carolina. The authors also acknowledge Jake Ragsdale for his assistance in producing graphics, especially in Fig. 1.

References

1 L. Langley, *How these animals use bubbles to their advantage, National Geographic*, 2019, **https://www.nationalgeographic.co.uk/animals/2019/05/how-these-animals-use-bubbles-to-their-advantage**.
2 R. Sheybani, H. Gensler and E. Meng, *Biomed. Microdevices*, 2013, **15**, 37–48.
3 D. Hua, A. Harizaj, M. Wels, T. Brans, S. Stremersch, H. De Keersmaecker, E. Bolea-Fernandez, F. Vanhaecke, D. Roels, K. Braeckmans, R. Xiong, C. Huang, S. C. De Smedt and F. Sauvage, *Adv. Mater.*, 2021, **33**, 2008379.
4 D. E. Lee, S. Soper and W. Wang, *Microsyst. Technol.*, 2008, **14**, 1751–1756.
5 L. Hsu, J. Ramunas, J. Gonzalez, J. Santiago and D. G. Strickland, *ECS Trans.*, 2019, **35**, 3–11.
6 W. Dong, M. Gauthier, C. Lenders and P. Lambert, *J. Micromech. Microeng.*, 2012, **22**, 057001.
7 L. Ren, R. H. Lee, H. R. Park, H. Ren, C. Nah and I.-S. Yoo, *J. Microelectromech. Syst.*, 2013, **22**, 1222–1228.
8 A. K. Han, S. Ji, D. Wang and M. R. Cutkosky, *IEEE Robot. Autom. Lett.*, 2020, **5**, 4021–4027.
9 R. S. Diteesawat, T. Helps, M. Taghavi and J. Rossiter, *Soft Rob.*, 2021, **8**, 186–199.
10 L. Jin, A. E. Forte and K. Bertoldi, *Adv. Sci.*, 2021, **8**, 2101941.
11 W. Carrigan, R. Stein, M. Mittal and M. B. J. Wijesundara, Conformal grasping using feedback controlled bubble actuator array, *Proc. SPIE 9116*, Next-Generation Robots and Systems, 911607, 2014, DOI: **10.1117/12.2058253**.
12 B. Mosadegh, P. Polygerinos, C. Keplinger, S. Wennstedt, R. F. Shepherd, U. Gupta, J. Shim, K. Bertoldi, C. J. Walsh and G. M. Whitesides, *Adv. Funct. Mater.*, 2014, **24**, 2163–2170.
13 R. F. Shepherd, A. A. Stokes, J. Freake, J. Barber, P. W. Snyder, A. D. Mazzeo, L. Cademartiri, S. A. Morin and G. M. Whitesides, *Angew. Chem.*, 2013, **125**, 2964–2968.
14 R. H. Heisser, C. A. Aubin, O. Peretz, N. Kincaid, H. S. An, E. M. Fisher, S. Sobhani, P. Pepiot, A. D. Gat and R. F. Shepherd, *Proc. Natl. Acad. Sci. U. S. A.*, 2021, **118**, e2106553118.
15 M. Duduta, E. Hajiesmaili, H. Zhao, R. J. Wood and D. R. Clarke, *Proc. Natl. Acad. Sci. U. S. A.*, 2019, **116**, 2476–2481.
16 T. Shay, O. D. Velev and M. D. Dickey, *Soft Matter*, 2018, **14**, 3296–3303.
17 V. Vallem, E. Roosa, T. Ledinh, W. Jung, T. Kim, S. Rashid-Nadimi, A. Kiani and M. D. Dickey, *Adv. Mater.*, 2021, 2103142.
18 H.-J. Koo, J.-H. So, M. D. Dickey and O. D. Velev, *Adv. Mater.*, 2011, **23**, 3559–3564.
19 Bubble, **Merriam-Webster.com** Dictionary, **https://www.merriam-webster.com/dictionary/bubble**, acessed 4 Mar. 2022.
20 A. Roux, A. Duchesne and M. Baudoin, *Phys. Rev. Fluids*, 2022, **7**, L011601.
21 M. Li, A. Pal, A. Aghakhani, A. Pena-Francesch and M. Sitti, *Nat. Rev. Mater.*, 2022, **7**, 235–249.
22 M. D. Dickey, *Adv. Mater.*, 2017, **29**, 1606425.
23 M. R. Khan, C. B. Eaker, E. F. Bowden and M. D. Dickey, *Proc. Natl. Acad. Sci. U. S. A.*, 2014, **111**, 14047–14051.
24 M. R. Khan, C. Trlica and M. D. Dickey, *Adv. Funct. Mater.*, 2015, **25**, 671–678.
25 M. R. Khan, J. Bell and M. D. Dickey, *Adv. Mater. Interfaces*, 2016, **3**, 1600546.
26 X. Liu, J. Liu, S. Lin and X. Zhao, *Mater. Today*, 2020, **36**, 102–124.
27 L. Ionov, *Mater. Today*, 2014, **17**, 494–503.
28 J.-S. Yoo and S.-M. Park, *Anal. Chem.*, 2000, **72**, 2035–2041.
29 D. E. Lee, S. Soper and W. Wang, Fabrication of a microfluidic system with integrated electrochemical pump and valves, *Proc. SPIE 6465*, Microfluidics, BioMEMS, and Medical Microsystems V, 64650B, 2007, DOI: **10.1117/12.713916**.

30 H. Lu, G. Yun, T. Cole, Y. Ouyang, H. Ren, J. Shu, Y. Zhang, S. Zhang, M. D. Dickey, W. Li and S.-Y. Tang, *ACS Appl. Mater. Interfaces*, 2021, **13**, 37904–37914.
31 A. M. Hubbard, W. Cui, Y. Huang, R. Takahashi, M. D. Dickey, J. Genzer, D. R. King and J. P. Gong, *Matter*, 2019, **1**, 674–689.
32 G. Alici, T. Canty, R. Mutlu, W. Hu and V. Sencadas, *Soft Rob.*, 2018, **5**, 24–35.
33 S. Chen, M. W. M. Tan, X. Gong and P. S. Lee, *Adv. Intell. Syst.*, 2022, **4**, 2100075.
34 X. Zhu, Y. Hu, G. Wu, W. Chen and N. Bao, *ACS Nano*, 2021, **15**, 9273–9298.
35 A. Le Duigou and M. Castro, *Sci. Rep.*, 2016, **6**, 18105.
36 C. A. Aubin, B. Gorissen, E. Milana, P. R. Buskohl, N. Lazarus, G. A. Slipher, C. Keplinger, J. Bongard, F. Iida, J. A. Lewis and R. F. Shepherd, *Nature*, 2022, **602**, 393–402.